Title
Variable Temperature Behaviour of the Hybrid Double Perovskite MA2KBiCl6

Journal
Molecules, 28(1)

ISSN
1420-3049

Authors
Wei, Fengxia
Wu, Yue
Sun, Shijing
et al.

Publication Date
2023

DOI
10.3390/molecules28010174

Peer reviewed

molecules

MDPI

Communication

Variable Temperature Behaviour of the Hybrid Double Perovskite MA_2KBiCl_6

Fengxia Wei [1,*], Yue Wu [2], Shijing Sun [3], Zeyu Deng [4], Li Tian Chew [1], Baisong Cheng [1], Cheng Cheh Tan [1], Timothy J. White [5] and Anthony K. Cheetham [4,6]

1 Institute of Materials Research and Engineering, Agency for Science, Technology and Research, 2 Fusionopolis Way, Singapore 138634, Singapore
2 Stanford Synchrotron Radiation Lightsource (SSRL), SLAC National Accelerator Laboratory, Menlo Park, CA 94025, USA
3 Energy and Materials Division, Toyota Research Institute, California, CA 94022, USA
4 Department of Materials Science and Engineering, National University of Singapore, Singapore 117575, Singapore
5 School of Materials Science and Engineering, Nanyang Technological University, 50 Nanyang Avenue, Singapore 639798, Singapore
6 Materials Research Laboratory, University of California, Santa Barbara, CA 93106, USA
* Correspondence: wei_fengxia@imre.a-star.edu.sg

Abstract: Perovskite-related materials show very promising properties in many fields. Pb-free perovskites are particularly interesting, because of the toxicity of Pb. In this study, hybrid double perovskite MA_2KBiCl_6 (MA = methylammonium cation) was found to have interesting variable temperature behaviours. Both variable temperature single crystal X-ray diffraction, synchrotron powder diffraction, and Raman spectroscopy were conducted to reveal a rhombohedral to cubic phase transition at around 330 K and an order to disorder transition for inorganic cage below 210 K.

Keywords: hybrid halide perovskite; phase transition; Pb-free

check for updates

Citation: Wei, F.; Wu, Y.; Sun, S.; Deng, Z.; Chew, L.T.; Cheng, B.; Tan, C.C.; White, T.J.; Cheetham, A.K. Variable Temperature Behaviour of the Hybrid Double Perovskite MA_2KBiCl_6. *Molecules* **2023**, *28*, 174. https://doi.org/10.3390/molecules28010174

Academic Editor: René M. Williams

Received: 8 December 2022
Revised: 21 December 2022
Accepted: 22 December 2022
Published: 25 December 2022

1. Introduction

In the past decades, solution-processable hybrid lead halide perovskites $MAPbX_3$ (MA = methylammonium cation, X = Cl, Br, I) have achieved a remarkable power conversion efficiency and photoluminescence quantum yield, finding their applications in many fields such as photovoltaics, X-ray detectors, LED, etc. [1–3] The search for lead-free alternatives has been the subject of much research in the last few years. Since 2016, making halide double perovskite via heterovalent substitution of Pb^{2+} by a monovalent cation (M^+) and environmental benign $Bi^{3+}/Sb^{3+}/In^{3+}$ provided a plausible approach, where the 3D perovskite framework is maintained by alternating corner-connected MX_6 and BiX_6 (or SbX_6, InX_6) octahedra. In the last century, inorganic double perovskites, i.e., elpasolites, have been systematically synthesized, and mostly with ionic Li, Na, F, and Cl which generally give wide bandgaps [4–6]. Within just one year, six new double perovskites that can be potential photovoltaic materials were reported—MA_2KBiCl_6 [7], $MA_2TlBiBr_6$ [8], $MA_2AgBiBr_6$ [9], $Cs_2AgBiCl_6$ [10,11], $Cs_2AgBiBr_6$ [12], and $Cs_2AgInCl_6$ [13], with optical bandgaps ranging from 1.9 eV to 3.3 eV. Later we discovered $Cs_2AgSbBr_6$ with a bandgap as low as 1.55 eV [14]. They showed remarkably similar physical properties with their lead analogues.

In this paper, we investigate the variable temperature behaviours of MA_2KBiCl_6, the first reported hybrid double perovskite, finding a reversible phase transition from $R\bar{3}m$ to $Fm\bar{3}m$ at 330 K. More complicated low temperature behaviour was detected from variable temperature (VT) single crystal and synchrotron powder X-ray diffraction and Raman spectroscopy.

2. Results and Discussions

2.1. High Temperature Phase Transition

At room temperature (RT), the MA_2KBiCl_6 crystal structure possesses rhombohedral symmetry $R\bar{3}m$ (No. 166), a = 7.8379(2) Å, c = 20.9801(6) Å (CCDC 145389), where the MA cations align along the *c* axis and corner-connecting octahedra tilted with K-Cl-Bi angle 173.04° (Figure 1). Both KCl_6 and $BiCl_6$ octahedra are slightly distorted [7].

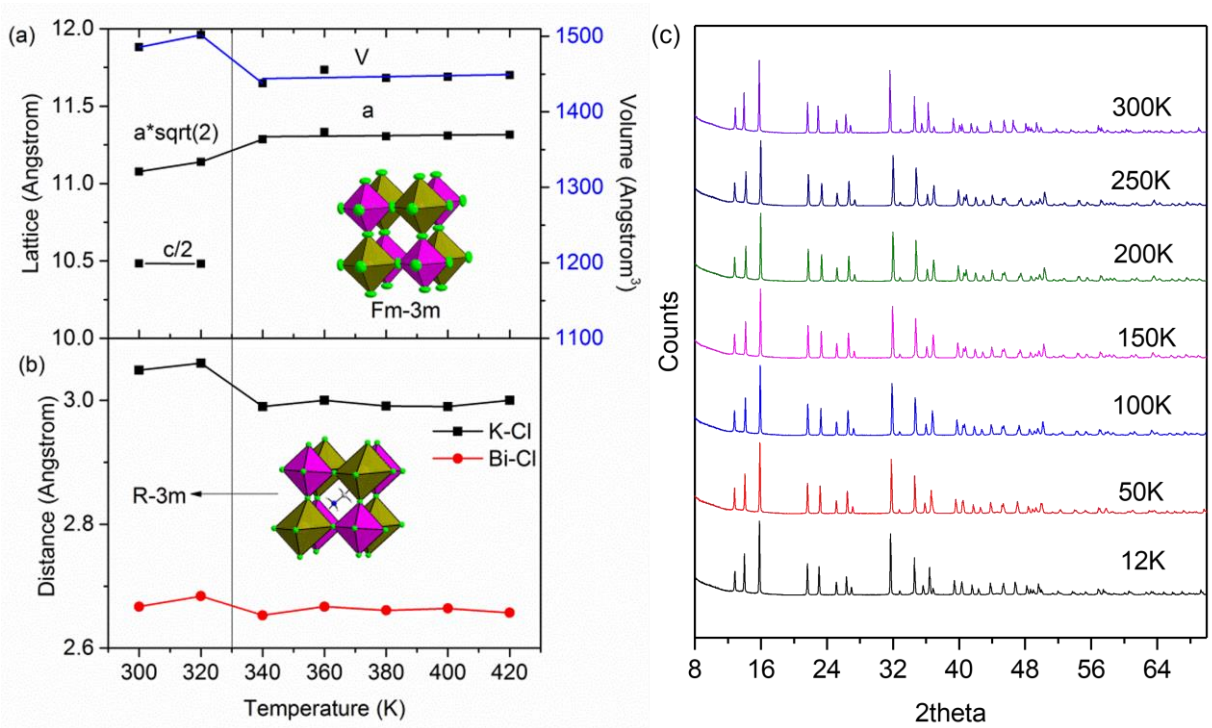

Figure 1. (**a**) Lattice parameters variations as a function of temperature. The lattice parameters of the rhombohedral cell were converted into its equivalent cubic setting. (**b**) Bond distance variations. Octahedral arrangements at both rhombohedral and cubic symmetry are illustrated (MA cation is omitted in cubic cell for illustration purpose. Green: Cl, purple $BiCl_6$, brown: KCl_6. (**c**) The VT synchrotron PXRD patterns.

Upon heating above 330K, a phase transition to typical halide double perovskite symmetry—cubic $Fm\bar{3}m$ (a = 11.4326(2) Å at 380 K, CCDC 2224436)—is seen and MA cations become disordered, similarly to their $MA_2AgBiBr_6$ counterpart [9] (Figures 1 and S1, Tables S1 and S2). The octahedra experience a transition from tilted to regular, yielding contractions in the K-Cl (~2.29%) and Bi-Cl (~1.15%) interatomic distances through the phase transition from 320 K to 340 K. KCl_6 shows a larger contraction due to the lower coulombic affinity between K^+ and Cl^- compared to Bi^{3+} and Cl^-, weaker Cl^- to Cl^- repulsion in the KCl_6 octahedron due to larger K^+ size, and less directional ionic bonds making the KCl_6 octahedron easier to rotate/distort. A similar phenomenon is observed in zeolites when substituting Zn^{2+} with Li^+ and B^{3+}—upon applying pressure, a larger distortion is observed around Li, which has lower valence and larger ionic size [15]. After the phase transition, further increasing temperature did not cause significant changes in bond lengths, lattice parameters, or unit cell volumes.

2.2. Low Temperature Behaviour

VT PXRD patterns from 300 K to 12 K did not show any peak splitting or abnormal peak broadening; anisotropic thermal expansion was detected by anisotropic peak shifting (Figure 1c). More detailed analysis was conducted by VT SCXRD. Upon cooling, negative and nonlinear thermal expansion along the c axis and continuous volume reduction can be

observed throughout the temperature range, and approximately linear thermal expansion 9.07×10^{-5} K^{-1} for the a axis is obtained until 190 K (Figure 2). A sudden change regarding the octahedral tilting and distance of hydrogen bond (Figure S2) below 230 K suggests possible phase transitions [16]. The LT structures are analysed based on the organic molecules and inorganic framework, respectively.

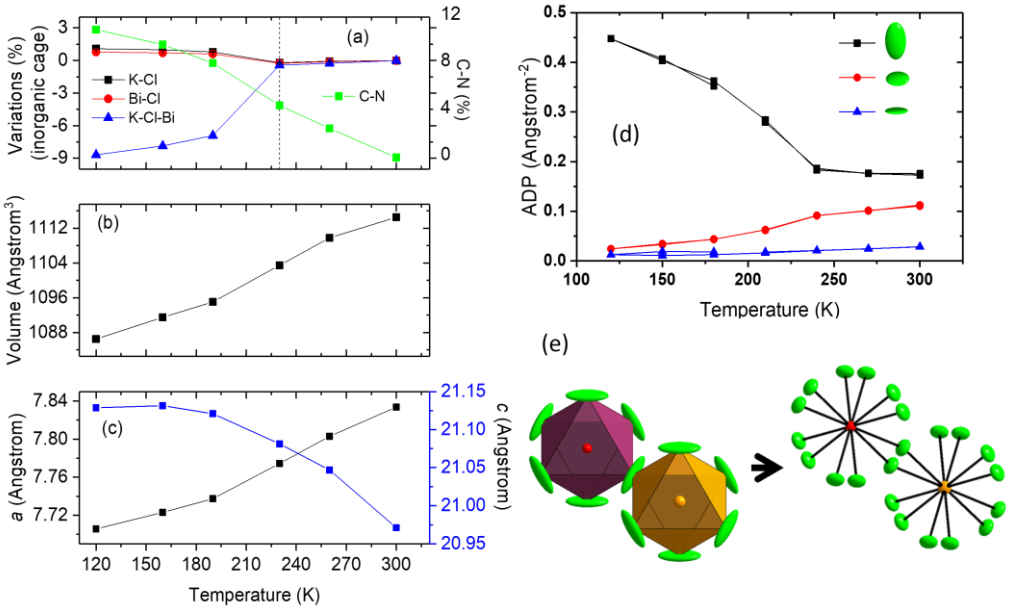

Figure 2. (**a**) Bond length and angle variations as function of temperature during cooling. Left axis: K-Cl, Bi-Cl bond lengths and K-Cl-Bi angle. Right axis: C-N distance. Both y axes show percentage changes from 225 K for easy comparison. (**b**) Volume and (**c**) lattice parameters expansion in response to temperature. (**d**) Cl anisotropic displacement parameters along the maximum, medium and minimum elongation directions. (**e**) The Cl splitting model. Data are from SCXRD.

The octahedral tilting, accompanied with distortion, has increased with lowering temperature, where larger distortion occurs again to KCl_6 (Figures 2 and S3), for similar reasons to the HT phase: that the larger octahedron with a cation of lower valence is more easily distorted. However, below 230 K, the anisotropy of Cl ellipsoids increases abruptly, where the ratio of the maximum, medium, and minimum values can reach ~ 35:2:1 at 120 K (Figure 2d). Symmetry reduction to other rhombohedral, orthorhombic, monoclinic, and even triclinic space groups have been attempted, but they either gave high residual electron density or failed. Hence, we propose a disordered model under the same space group $R\bar{3}m$ with Cl split into two symmetrical equivalent positions, with each having 50% occupancy (Table S5 and Figure 2e). From SCXRD, we are able to narrow down the transition range to between 210 K to 190 K.

VT Raman spectroscopy further proves the retention of symmetry, as no extra peaks or peak splitting was observed (Figure 3) [17]. Raman spectra were collected from RT to 120 K at a laser wavelength of 532.05 nm. Four peaks are present from 50 cm^{-1} to 350 cm^{-1}, similar to its inorganic analogue, $Cs_2NaBiCl_6$ [17]. The possible assignments of frequencies are (1) the stretching of Cl atoms towards and away from the central Bi/K atoms, (2) 3 Cl atoms away from Bi/K and 3 Cl towards central atoms in the octahedron at the same time, (3) octahedral bending and (4) lattice mode of MA cations, from high to low wave numbers, respectively [18].

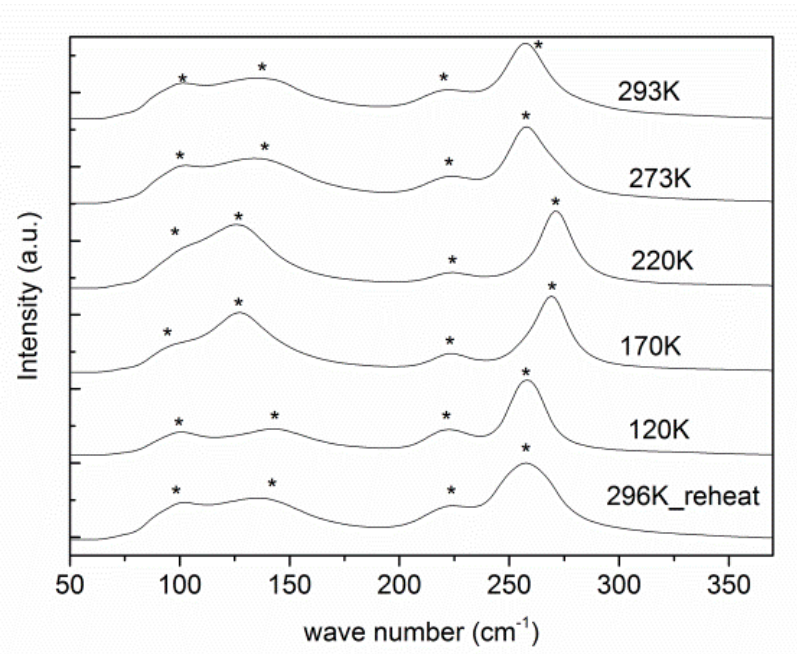

Figure 3. VT Raman spectra during cooling for $(MA)_2KBiCl_6$. The peaks are highlighted by *.

Although the MA cations seem to be crystallographically ordered at RT, the short C-N bonds (1.32 Å) suggest otherwise, as the anisotropic thermal ellipsoids for both C and N indicate strong transverse vibrations resulting from relatively high molecular mobility. Upon cooling, the MA molecules tend to be frozen, shown as the increasing crystallographic C-N distances (Figures 1 and 4), which provide the major contribution to the negative thermal expansion of c axis. When further inspecting the ellipsoids, the N vibrations tend to become isotropic, and anisotropy of C also decreases yet is still present, which we speculate is due to the change of MA vibrational modes. Figure 4 provides an illustration, of the possible vibrational modes of the MA molecule. At RT, the centre of mass serves as the centre of liberation, yielding similar ellipsoids for C and N. As temperature is reduced, the liberation centre moves towards N, most likely due to the locking-in of hydrogen bonds between N-H···Cl. Similar behaviours can be expected in the rare earth double perovskites MA_2KYCl_6 and MA_2KGdCl_6 [19].

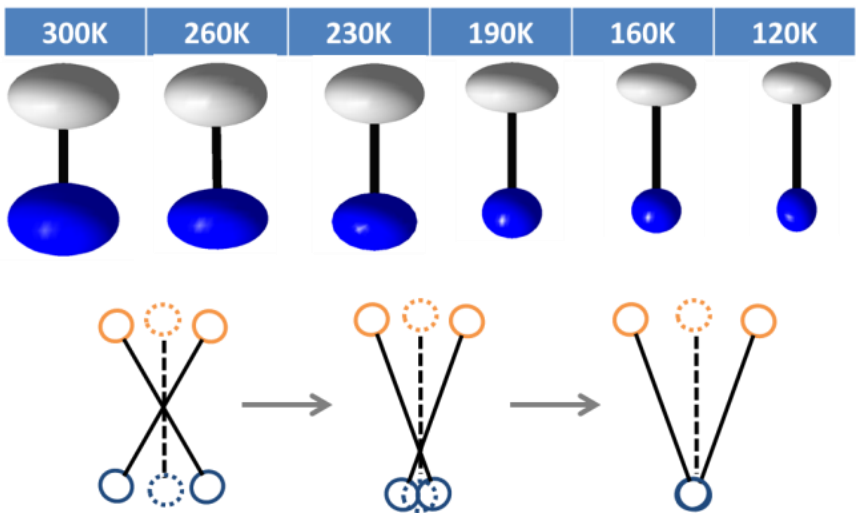

Figure 4. C-N thermal ellipsoids (at 50% probability) and the possible vibration modes of MA at different temperatures. Grey and brown: C, blue: N.

3. Materials and Methods

Single crystal growth: A saturated solution of MACl (MA: methylammonium), KCl and bismuth acetate (molar ratio 2:1:1) in aqueous HCl (37 wt%) was prepared at 50 °C, then stored at 4 °C. Crystals of millimetre size were obtained using vacuum filtration after 7 days.

Single crystal structure determination from 120 K to 380 K was using an Oxford Gemini E Ultra diffractometer, Mo Kα radiation (λ = 0.71073Å), equipped with an Eos CCD detector. Diffractions at variable temperatures were performed by collecting data from 300 K to 120 K using Cryostream system with N_2 flow with 40 K steps, then heated up to 380 K for high temperature structure investigation. The crystal stayed under nitrogen flow for a further 30 min at each temperature to allow sufficient equilibration. Data collection and reduction were using CrysAliPro (Agilent Technologies). An empirical absorption correction was applied, and the structure was solved using ShelXS and refined by ShelXL with the Olex2 platform, except for the structure at 180 K, which was solved using Superflip and refined by JANA.

Raman spectra were recorded using a LabRam 300 Raman spectrometer coupled with an Olympus BXFM ILHS confocal microscope with 10 times and 50 times magnification available. The laser wavelength used was 532.05 nm; the laser power was kept at 100 mW for the duration of experimentation. The system was calibrated against the 520.5 cm Raman band of a crystalline silicon wafer. The sample holder and cooling stage was a Linkam Scientific DSC600 with associated liquid nitrogen pump. Variable temperature Raman was performed under an air atmosphere. A polycrystalline powder sample was placed in the sample holder/cooling stage which was subsequently sealed. The stage temperature was decreased by 10 K/min, and the sample was allowed to equilibrate at a given temperature for approximately 10 min before the collection of Raman spectra. After data collection at ~120 K, the sample was reheated at 10 K/min to room temperature 296 K, at which point Raman spectra were again recorded.

4. Conclusions

The Pb-free hybrid double perovskite MA_2KBiCl_6 was found to have interesting variable temperature behaviour. Upon heating to 330 K, a phase transition from $R\bar{3}m$ to $Fm\bar{3}m$ occurs, where the MA cations disorder to the cubic symmetry. At low temperatures, although synchrotron powder diffraction did not indicate any sign of phase transitions, the inorganic cage tended to be disordered below 210 K. The short C-N bond at room temperature is a manifestation of vibrational disorder.

Supplementary Materials: The following supporting information can be downloaded at: https://www.mdpi.com/article/10.3390/molecules28010174/s1, Figure S1. The crystal structure of MA_2KBiCl_6 double perovskite at 380 K; Figure S2: Distance of NH . . . Cl as a function of temperature; Figure S2: Octahedral angles variation with respect to temperature. Only one set of angles for each octahedra are shown (the total angle = 180° when plus the other set of angles). Smaller angle away from 90° means more distortion. Table S1: Atomic coordinates and ADPs at 380K; Table S2: Experimental details for HT phase (refinement using OLEX2); Table S3: Bond lengths at different temperatures; Table S4: Experimental details for LT phase, refinement using JANA; Table S5: Atomic coordinates and ADPs at 180 K [20–22].

Author Contributions: F.W.: Conceptualization, investigation, and writing, Y.W., S.S. and Z.D.: investigation and visualization, L.T.C., B.C. and C.C.T.: investigation, T.J.W. and A.K.C.: Conceptualization, review, and editing. All authors have read and agreed to the published version of the manuscript.

Funding: This work is funded by the career development fund from Agency for Science, Technology and Research (A*STAR), Singapore, grant number: C210112054.

Institutional Review Board Statement: Not applicable.

Informed Consent Statement: Not applicable.

Data Availability Statement: All data are available upon reasonable request from corresponding author.

Acknowledgments: The variable temperature powder diffraction data was collected at DIAMOND synchrotron light source, UK.

Conflicts of Interest: The authors declare no conflict of interest.

Sample Availability: Samples of the compounds are available from the authors.

References

1. Kojima, A.; Teshima, K.; Shirai, Y.; Miyasaka, T. Organometal Halide Perovskites as Visible-Light Sensitizers for Photovoltaic Cells. *J. Am. Chem. Soc.* **2009**, *131*, 6050–6051. [CrossRef] [PubMed]
2. National Renewable Energy Labs (NREL) Efficiency Chart. Available online: http://www.nrel.gov/ncpv/images/efficiency_chart.jpg (accessed on 25 July 2016).
3. Pan, W.; Wu, H.; Luo, J.; Deng, Z.; Ge, C.; Chen, C.; Jiang, X.; Yin, W.J.; Niu, G.; Zhu, L.; et al. Cs2AgBiBr6 Single-Crystal X-Ray Detectors with a Low Detection Limit. *Nat. Photon.* **2017**, *11*, 726–732. [CrossRef]
4. Morss, L.R.; Siegal, M.; Stenger, L.; Edelstein, N. Preparation of Cubic Chloro Complex Compounds of Trivalent Metals: Cs2NaMCl6. *Inorg. Chem.* **1970**, *9*, 1771–1775. [CrossRef]
5. Flerov, I.N.; Gorev, M.V.; Aleksandrov, K.S.; Tressaud, A.; Grannec, J.; Couzi, M. Phase Transitions in Elpasolites (Ordered Perovskites). *Mater. Sci. Eng. R Rep.* **1998**, *24*, 81–151. [CrossRef]
6. Couzi, M.; Khaïroun, S.; Tressaud, A. Structural Phase Transitions in Rb2KMIIIF6 Elpasolites. II. Raman Scattering and Group-Theoretical Studies of Rb2KFeF6 and Rb2KYF6. *Phys. Status Solidi (a)* **1986**, *98*, 423–434. [CrossRef]
7. Wei, F.; Deng, Z.; Sun, S.; Xie, F.; Kieslich, G.; Evans, D.M.; Carpenter, M.A.; Bristowe, P.D.; Cheetham, A.K. The Synthesis, Structure and Electronic Properties of a Lead-Free Hybrid Inorganic-Organic Double Perovskite (MA)2KBiCl6 (MA = Methylammonium). *Mater. Horiz.* **2016**, *3*, 328–332. [CrossRef]
8. Deng, Z.; Wei, F.; Sun, S.; Kieslich, G.; Cheetham, A.K.; Bristowe, P.D. Exploring the Properties of Lead-Free Hybrid Double Perovskites Using a Combined Computational-Experimental Approach. *J. Mater. Chem. A Mater.* **2016**, *4*, 12025–12029. [CrossRef]
9. Wei, F.; Deng, Z.; Sun, S.; Zhang, F.; Evans, D.M.; Kieslich, G.; Tominaka, S.; Carpenter, M.A.; Zhang, J.; Bristowe, P.D.; et al. Synthesis and Properties of a Lead-Free Hybrid Double Perovskite: (CH3NH3)2AgBiBr6. *Chem. Mater.* **2017**, *29*, 1089–1094. [CrossRef]
10. McClure, E.T.; Ball, M.R.; Windl, W.; Woodward, P.M. Cs2AgBiX6(X = Br, Cl): New Visible Light Absorbing, Lead-Free Halide Perovskite Semiconductors. *Chem. Mater.* **2016**, *28*, 1348–1354. [CrossRef]
11. Volonakis, G.; Filip, M.R.; Haghighirad, A.A.; Sakai, N.; Wenger, B.; Snaith, H.J.; Giustino, F. Lead-Free Halide Double Perovskites via Heterovalent Substitution of Noble Metals. *J. Phys. Chem. Lett.* **2016**, *7*, 1254–1259. [CrossRef]
12. Slavney, A.H.; Hu, T.; Lindenberg, A.M.; Karunadasa, H.I. A Bismuth-Halide Double Perovskite with Long Carrier Recombination Lifetime for Photovoltaic Applications. *J. Am. Chem. Soc.* **2016**, *138*, 2138–2141. [CrossRef] [PubMed]
13. Volonakis, G.; Haghighirad, A.A.; Milot, R.L.; Sio, W.H.; Filip, M.R.; Wenger, B.; Johnston, M.B.; Herz, L.M.; Snaith, H.J.; Giustino, F. Cs 2 InAgCl 6: A New Lead-Free Halide Double Perovskite with Direct Band Gap. *J. Phys. Chem. Lett.* **2017**, *8*, 772–778. [CrossRef] [PubMed]
14. Wei, F.; Deng, Z.; Sun, S.; Hartono, N.T.P.; Seng, H.L.; Buonassisi, T.; Bristowe, P.D.; Cheetham, A.K. Enhanced Visible Light Absorption for Lead-Free Double Perovskite Cs2AgSbBr6. *Chem. Communicat.* **2019**, *55*, 3721–3724. [CrossRef]
15. Bennett, T.D.; Tan, J.-C.; Moggach, S.A.; Galvelis, R.; Mellot-Draznieks, C.; Reisner, B.A.; Thirumurugan, A.; Allan, D.R.; Cheetham, A.K. Mechanical Properties of Dense Zeolitic Imidazolate Frameworks (ZIFs): A High-Pressure X-Ray Diffraction, Nanoindentation and Computational Study of the Zinc Framework Zn(Im)2, and Its Lithium—Boron Analogue, LiB(Im)4. *Chem. Eur. J.* **2010**, *16*, 10684–10690. [CrossRef] [PubMed]
16. Lu, W.; Song, W.D.; He, K.; Chai, J.; Sun, C.; Chow, G.; Chen, J. The role of octahedral tilting in the structural phase transition and magnetic anisotropy in SrRuO3 thin film. *J. Appl. Phys.* **2013**, *113*, 063901. [CrossRef]
17. Smit, W.M.A.; Dirksen, G.J.; Stufkens, D.J. Infrared and Raman Spectra of the Elpasolites Cs2NaSbCl6 and Cs2NaBiCl6: Evidence for a Pseudo Jahn-Teller Distorted Ground State. *J. Phys. Chem. Solids* **1990**, *51*, 189–196. [CrossRef]
18. Pistor, P.; Meyns, M.; Guc, M.; Wang, H.; Marques, M.; Alcobé, X.; Cabot, A.; Izquierdo-Roca, V. Advanced Raman spectroscopy of Cs2AgBiBr6 double perovskites and identification of Cs3Bi2Br9 secondary phases. *Scr. Mater.* **2020**, *184*, 24–29. [CrossRef]
19. Deng, Z.; Wei, F.; Brivio, F.; Wu, Y.; Sun, S.; Bristowe, P.D.; Cheetham, A.K. Synthesis and Characterization of the Rare-Earth Hybrid Double Perovskites: (CH3NH3)2KGdCl6 and (CH3NH3)2KYCl6. *J. Phys. Chem. Lett.* **2017**, *8*, 5015–5020. [CrossRef]
20. Dolomanov, O.V.; Bourhis, L.J.; Gildea, R.J.; Howard, J.A.; Puschmann, H. OLEX2: A Complete Structure Solution, Refinement and Analysis Program. *J. Appl. Cryst* **2009**, *42*, 339–341. [CrossRef]

21. Sheldrick, G. SHELXS97, Program for the Solution of Crystal Structures. *A short Hist. SHELX* **2008**, *64*, 112–122.
22. Sheldrick, G.M. Crystal Structure Refinement with SHELXL. *Acta Crystallogr. Sect. C Struct. Chem.* **2015**, *71*, 3–8. [CrossRef] [PubMed]